B — 6 — 2   New Coupled-Waveguide Optical Modulators with Schottky Contacts

K. Tada and H. Yanagawa*

Dept. of Electronic Engrg., Univ. of Tokyo (*Furukawa Electric Co.)

7-3-1 Hongo, Bunkyo-ku, Tokyo, 113 Japan

The coupled-waveguide optical modulator/switch will be one of essential components in integrated optical circuits. This type of device was first realized in a GaAs multilayered planar waveguide configuration[1]. Several kinds of this device in $Al_xGa_{1-x}As$ channel waveguide configurations have also been reported so far[2-5]. In this paper we propose two new device structures with Schottky contacts in embedded-waveguide and rib-waveguide configurations and report the realization of GaAs homostructured rib-waveguide modulators with some experimental results.

Schematic diagrams of these modulators are shown in Figs. 1 and 2. The device shown in Fig. 1 is composed of an n^+-$Al_xGa_{1-x}As$ substrate, an n-GaAs guide layer, an n-$Al_yGa_{1-y}As$ buffer layer and Al schottky contacts. Diffusion or ion implantation of donors into the dotted area is necessary so as to obtain built-in refractive index difference in horizontal directions due to the free carrier effect. Thus both optical and modulating fields are confined mainly in the guide layer beneath the electrodes and efficient modulation is expected because of large overlap of both fields. The second device illustrated in Fig. 2 consists of an n^+-$Al_xGa_{1-x}As$ substrate, n-GaAs guide layer and Al schottky contacts, and two rib-waveguides are formed by a suitable etching process. In this device also, both optical and modulating fields are confined mainly in the guide layer beneath the ribs and this results in efficient modulation.

These two devices were analyzed by applying an equivalent refractive index method and dependence of their characteristics on device parameters was studied. Numerical calculations based on this analysis were carried out at the light wavelength of 1.06μm in E_{11}^x optical mode (TE-like fundamental mode). We designed a number of devices considering practical limitations restricted from the present fabrication technology based on the epitaxial growth and the photolithographic process. Examples of results are tabulated in TABLEs 1 and 2 for embedded-waveguide devices and rib-waveguide ones, respectively. It is shown that the heterostructured embedded-waveguide device is suitable for efficient modulation and that the homostructured rib-waveguide device has fairly small modulating power per bandwidth P/Δf in spite of its simpler structure.

With these results in mind experimental samples were fabricated to show the feasibility of the rib-waveguide device. The wafer used in the experiment was originally for Gunn diode. It had two vapor-phase epitaxially grown layers; an n^+-GaAs buffer layer (5.5 $\times 10^{17} cm^{-3}$, 10.5μm) on n^+-GaAs substrate and an n^--GaAs guide layer (1.3 $\times 10^{15} cm^{-3}$, 5.0μm) on the buffer layer. The rib-waveguides were formed by etching Al in H_3PO_4 and then GaAs in $3H_2SO_4 + 1H_2O_2 + 6H_2O$). The measured widths of the rib tops and bottoms are 2.7 and 4.7μm, and spacings between them are 5.0μand 3.6μm respectively. Etched depth (t in TABLE 2) is 2.0μm.

One of the samples with L of 3.9 mm was evaluated at 1.06μm light wavelength using the end-fire coupling scheme. The optical power output from each waveguide is measured as a function of applied dc reverse voltage V (The break-down voltage was about 31V). Using the well-known coupled-mode formalism, the data obtained are fitted to the following theoretical curve,

$$I_2 /(I_1 + I_2) = (\sin DcL / D)^2 \quad (1), \qquad D = \{1 + (V - V_B)^2 / V_A^2\}^{1/2} \quad (2)$$

where I_1, I_2 : output power from excited and non-excited and waveguides respectively, c: coupling coefficient, V_A, V_B : fitted parameters. The parameters determined are : c=0.32mm^{-1}, V_A =31V, and V_B=5V. From these the coupling length L (=π/2c) of 4.9mm and switching voltage $V_s\{\equiv V(I_2=0)-V_B\}$ of 72V are determined. They are in fair agreement with those (L =3.7mm, V_s=79V for L=3.9mm) obtained from the theoretical analysis where the rib width and spacing are evaluated at the rib bottoms. The low V_B of 5V for maximum output from the non-excited guide indicates that two guides are highly synchronous; the relative difference in the phase constants Δβ/β is very small ($\approx 5 \times 10^{-6}$).

The insertion loss was measured to be about 20dB and it seems to be mainly due to roughness of etched and cleaved surface of the waveguides. Improvement of this device is under way and the results will be reported further.

The authors gratefully acknowledge Drs. W. Susaki, M. Ishii and C. Kimura for supplying wafers, Prof. M. Aoki and Dr. K. Hirose for valuable discussions, and Messrs. Y. Matsunaga and Y. Hirayama for their assistance in experiments.

REFERENCES; (1) K. Tada and K. Hirose: Appl. Phys. Lett. 25, 561 (1974); Proc. 6th Conf. Solid State Devices, Tokyo (1975). (2) J.C. Campbell et al: Appl. Phys. Lett. 27, 202 (1975). (3) F.J. Leonberger et al: Appl. Phys. Lett. 29, 652 (1976). (4) F.K. Reinhart et al: Tech. Digest 1977 Int. Conf. Integrated Optics and Optical Fiber Commun. p-11, Tokyo (1977). (5) K. Tada et al: Trans. Inst. Electron. Commun. Engr. Japan, E61, 1 (1978).
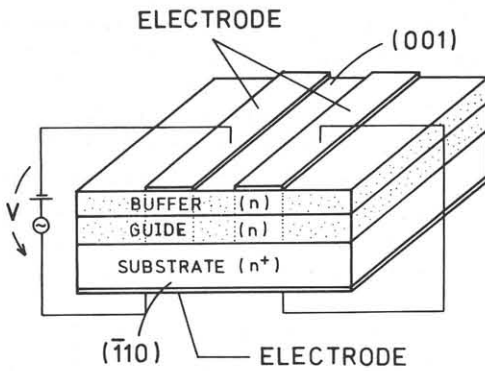
Fig. 1 The coupled-waveguide optical modulator in embedded-waveguide configuration.
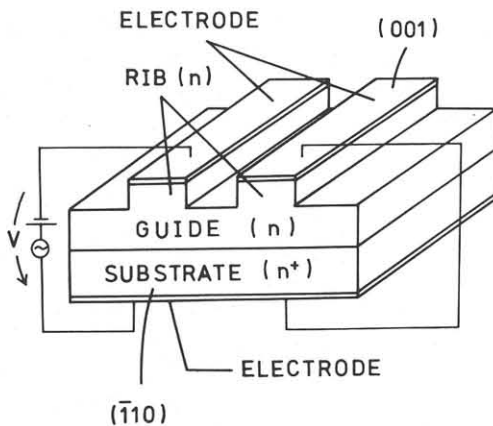
TABLE 1   Design examples of $n^+Al_xGa_{1-x}As$-n GaAs-n $Al_yGa_{1-y}As$ -Al embedded-waveguide modulator (E_{11}^x mode, $\lambda_0 = 1.06\mu m$ and $V_{BIAS} = 20V$. Built-in refractive index difference of the embedded-waveguide in horizontal direction is assumed to be 3.48×10^{-4}). Optical absorption loss due to electrode is negligibly small.

		1	2	3
CARRIER CONCENTRATION				
IN BUFFER	(cm^{-3})	10^{15}	10^{15}	10^{15}
IN GUIDE	(cm^{-3})	10^{15}	10^{15}	10^{15}
IN SUBSTRATE	(cm^{-3})	5×10^{17}	10^{18}	10^{18}
COMPOSITION RATIO x,y OF BUFFER AND SUBSTRATE		0.07	0.07	0.07
ELECTRODE WIDTH	w (μm)	4	4	4.5
ELECTRODE SPACING	d (μm)	5	4	4.5
BUFFER THICKNESS	t (μm)	0.2	0.2	0.2
GUIDE THICKNESS	h (μm)	1.2	0.8	1
DEVICE LENGTH	L(=L_0) (mm)	4.0	3.3	3.9
BARRIER CAPACITANCE C (pF)		1.2	1.4	1.5
MODULATION VOLTAGE FOR 100% MODULATION V_0 (peak value) (V)		10.2	11.0	7.6
BANDWIDTH	Δf (GHz)	5.5	4.7	4.3
P/Δf (100%)	$(\mu W/MHz)$	190	258	133

Fig. 2 The coupled-waveguide optical modulator in rib-waveguide configuration.

TABLE 2   Design examples of n^+ $Al_xGa_{1-x}As$-n GaAs-Al rib-waveguide modulator (E_{11}^x mode, $\lambda_0 = 1.06\mu m$, $V_{BIAS} = 40V$ for example 1 and $V_{BIAS} = 20V$ for examples 2 and 3).

		1	2	3
CARRIER CONCENTRATION				
IN GUIDE	(cm^{-3})	10^{15}	10^{15}	10^{15}
IN SUBSTRATE	(cm^{-3})	4.5×10^{18}	10^{18}	10^{18}
COMPOSITION RATIO x OF SUBSTRATE		0	0.04	0.07
RIB WIDTH	w (μm)	4	4	3
RIB SPACING	d (μm)	4	3	4
RIB HEIGHT	t (μm)	1	0.2	0.1
GUIDE THICKNESS	h (μm)	3	1	0.9
DEVICE LENGTH	L(=L_0) (mm)	3.7	3.8	3.6
BARRIER CAPACITANCE C_B (pF)		0.41	1.4	1.2
MODULATING VOLTAGE FOR 100% MODULATION V_0 (peak value) (V)		20.6	6.9	6.4
BANDWIDTH	Δf (GHz)	15.7	4.6	5.4
P/Δf (100%)	$(\mu W/MHz)$	270	103	77
ABSORPTION LOSS DUE TO ELECTRODE (dB)		0.3	3.8	9.9